Electronic Supplementary Information for

Efficient sewage sludge-derived bi-functional electrocatalyst for oxygen reduction and evolution reaction

Shi-Jie Yuan, Xiao-Hu Dai*

State Key Laboratory of Pollution Control and Resource Reuse, College of Environmental Science and Engineering, Tongji University, Shanghai, 200092, China

***Corresponding author:**

Prof. Xiao-Hu Dai, Phone: +86-21-65986297; Fax: +86-21-65983602; E-mail: daixiaohu@tongji.edu.cn

The effect of N, Fe and S components

It was found that the SN-AW shows enhanced N content of SN-AW (1.84%) by NH_3 atmosphere, compared with that of SS-AW (1.10%). The enhanced N content of SN-AW, accompanied with a high percentage of pyridinic-N (25.7%/N) and graphitic-N (33.4%/N) dopants which are known to decrease the over-potentials of ORR, was assumed to facilitate the adsorption and dissociation of O_2 and OH^- and thus promote electron transfer. This fact clearly indicates that the improved performance of SN-AW with larger steady-state current density compared with that of SS-AW could attributed to the enhanced N content with the NH_3 atmosphere as nitrogen dopants (Figure S4a).

The ORR activity of SN-AW in 0.1 M KOH containing 10 m M CN^-, which is known to coordinate strongly to Fe and poison the Fe-centred catalytic sites for ORR[S1], was investigated to assess the role of Fe in forming active ORR catalytic sites on the sewage sludge-derived carbon-based catalysts (Figure S4a). In the present of the CN^-, the onset potential of the SN-AW catalyst decreases by 0.05 V, with a significantly decrease in the steady-state current density, suggesting blocking of the Fe-centred catalytic sites by CN^- ions. This result clearly clarifying that Fe species were also important to the high ORR catalytic activity observed in the as-synthesized SN-AW.

In order to assess the role of S in improving the catalytic activity of the SN-AW, the sewage sludge was pretreated with 0.1 M HCl to decrease the S content. With the addition of HCl, the S content in the sewage sludge could be partly released in the

form of H_2S, a poisonous gas that smells like rotten eggs. Stoichiometric ammonium hydroxide was added to restore the pH value of the sewage sludge. Then the pretreatment sewage sludge was annealed in NH_3 atmosphere following the same steps to obtain the sludge-derived carbon-based catalyst SN-AW-S. Accompanied with a decreased of the S content from 0.45% to 0.38%, a small negative shift of the onset potential and steady-state current density was obtained when compared with that of SN-AW, indicating the role of S content in improving the catalytic activity of the SN-AW (Figure S4a).

Furthermore, the higher onset potential of the SN-AW compared with those of SS-AW, SN-AW-CN, and SN-AW-S suggest a synergetic effect between the N, Fe, and S components (Figure S4a). Especially, the much lower onset potential of the SS-AW and SN-AW-CN suggests that the complex of the doped-N, -Fe, and carbon atoms might be one kinds of the active sites on the SN-AW. The new complex active site, which possesses much higher intrinsic activity for ORR than a single N- or Fe-doped active site, is most probably the in-plane Fe-N_4 centers embedded in a graphene-type matrix which can activate the ORR process by the significant decrease of oxygen adsorption energy and extension of the O-O bond according to quantum calculation [S1].

Features of the as-synthesized SN-AW in our work

Actually, as being observed in Table S2, although several kinds of sludge/biomass-derived carbon material as electrocatalysts in the alkaline media been

reported, our work is the first report of a sewage sludge-derived multi-doped porous carbon material with highly efficient activity for bi-functional ORR and OER catalysis, especially for ORR in acidic media which is rare property for sludge/biomass-derived electrocatalysts and even synthesized electrocatalysts derived from chemicals precursors.

None of the previously reported sludge-derived electrocatalysts showed some OER activity or ORR activity in acidic media [S2-S5]. And very few reported non-Pt electrocatalysts derived from chemicals precursors showed high performance for ORR in both alkaline and acidic medium in the present (Table S2). In contrast, the ORR electrocatalytic performance of the as-synthesized carbon material in our work compares favorably with the commercial 20% Pt/C catalyst in both acidic and basic media. These features make the as-synthesized carbon material in our work very attractive as an ORR catalyst for many important energy conversion and storage technologies that typically proceed in acidic media.

References

S1 K. Ai, Y. Liu, C. Ruan, L. Lu, G. M. Lu, *Adv. Mater*. 2013, 25, 998-1003.

S2 K. Zhou, W. Zhou, X. Liu, Y. Wang and J. Wan, S. Chen, *ACS Appl Mater. Interfaces* 2014, 6, 14911-14918.

S3 Y. Yuan, T. Yuan, D. Wang, J. Tang, S. Zhou. *Bioresource Technol*. 2013, 144, 115-120.

S4 Y. Yuan, T. Liu, P. Fu, J. Tang, S. Zhou, *J. Mater. Chem. A* 2015, 3, 8475-8482.

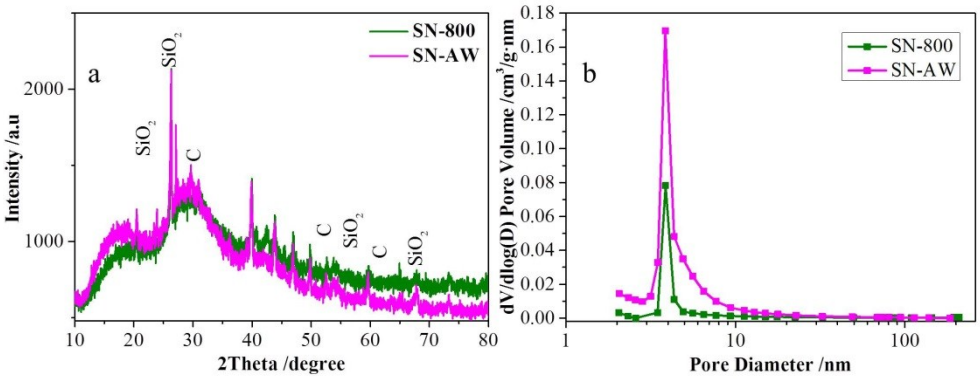

Fig. S1 XRD spectrum (a) and pore size distributions (b) of the SN-800 and SN-AW.

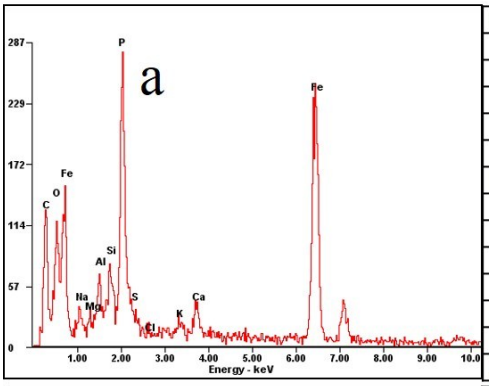

Element	Wt%	At%
CK	37.97	62.36
OK	11.61	14.32
NaK	1.01	0.86
MgK	0.62	0.50
AlK	2.04	1.49
SiK	2.13	1.49
PK	9.57	6.10
SK	0.64	0.39
ClK	0.10	0.06
KK	0.59	0.30
CaK	1.55	0.76
FeK	32.17	11.36
Matrix	Correction	ZAF

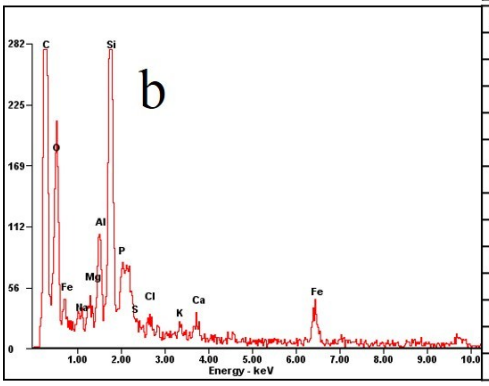

Element	Wt%	At%
CK	65.42	76.75
OK	17.91	15.78
NaK	0.50	0.31
MgK	0.55	0.32
AlK	2.04	1.06
SiK	7.06	3.54
PK	1.68	0.76
SK	0.45	0.20
ClK	0.40	0.16
KK	0.41	0.15
CaK	0.63	0.22
FeK	2.95	0.75
Matrix	Correction	ZAF

Fig. S2 Energy dispersive X-ray (EDX) spectra of the SN-800 (a) and SN-AW (b).

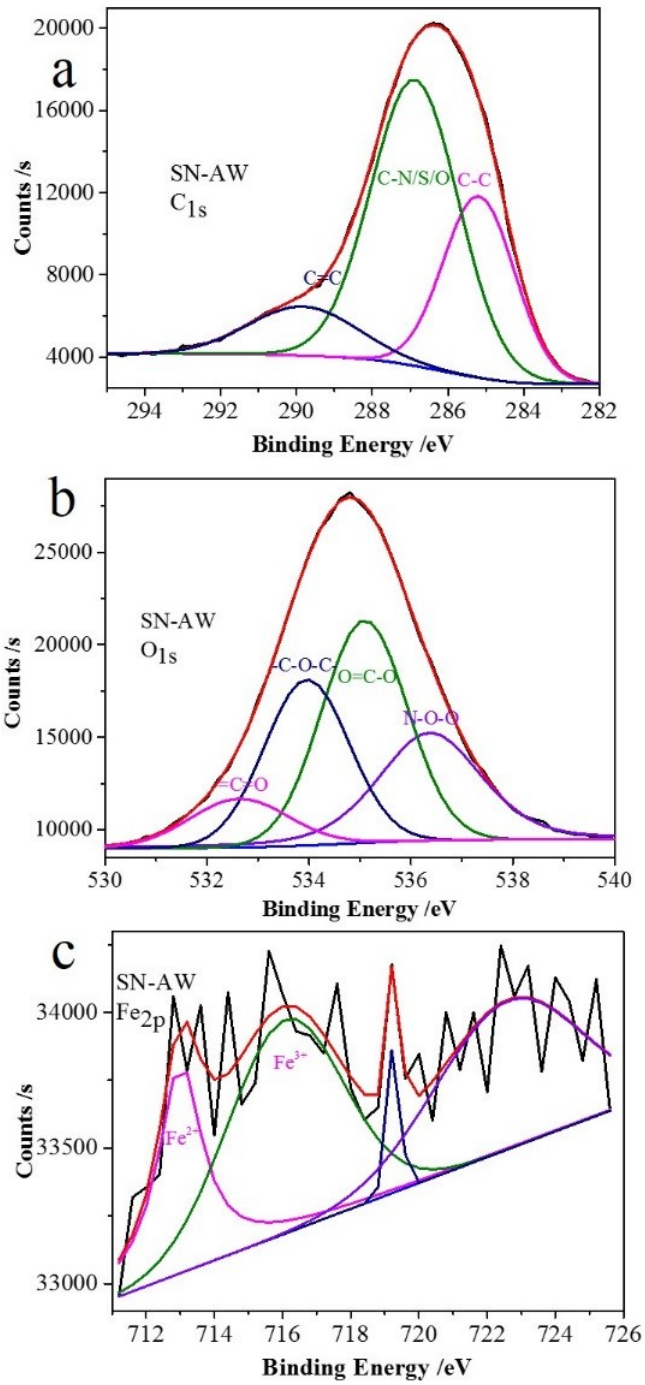

Fig. S3 The high resolution C 1s (a), O 1s (b), and Fe 1s (c) XPS spectra of the SN-AW.

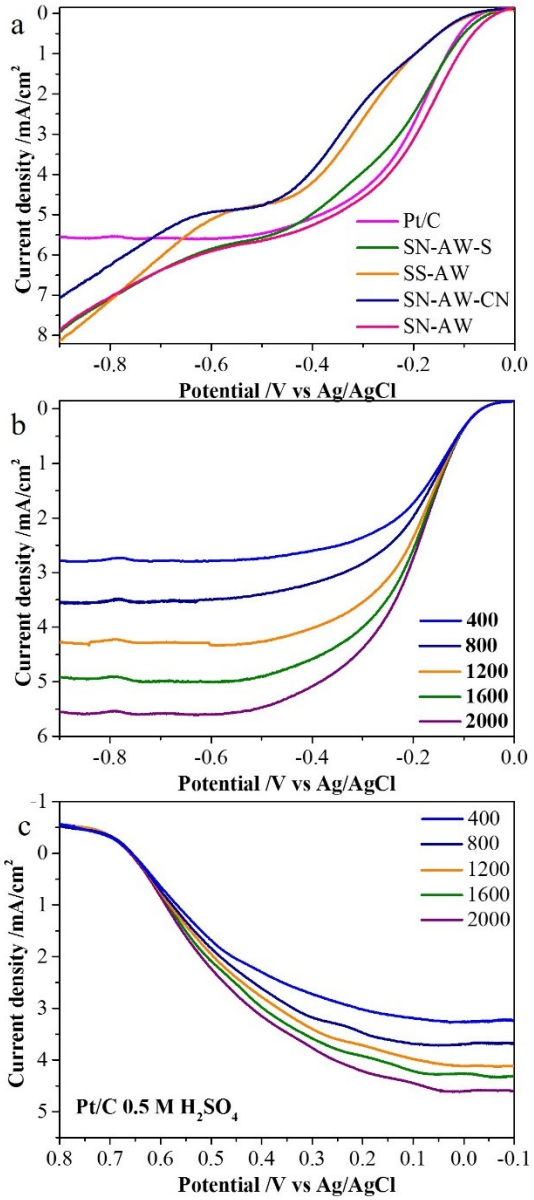

Fig. S4 LSV curves of SN-AW, SS-AW, SN-AW-S (the sewage sludge pretreatment with HCl to partly remove the S content and then annealed in NH_3 atmosphere), and commercial Pt/C catalysts in O_2-saturated 0.1 M KOH solutions, and LSV curves of SN-AW in O_2-saturated 0.1 M KOH containing 10 mM KCN (SN-AW-CN) (a), LSV curves of commercial Pt/C catalysts with different rotation speed in O_2-saturated 0.1 M KOH solutions (a) and 0.5 M H_2SO_4 solutions at the scan rate of 5 mV s^{-1} with different rotation speed.

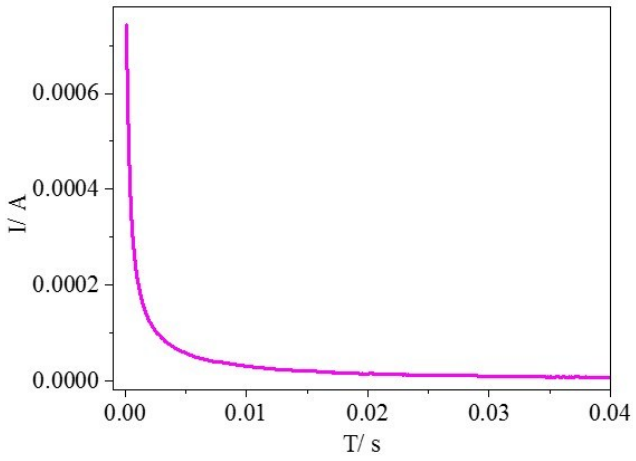

Fig. S5 Chronoamperometry curve of the as-synthesized SN-AW electrode in 1.0×10^{-4} M $K_3[Fe(CN)_6]$ with 1 M KCl.

The catalytic active surface area was investigated by chronoamperometry method (Kinoshita et al. Modern aspects of electrochemistry. Chapter 4. "Preparation and Characterization of Highly Dispersed Electrocatalytic Materials" New York 1977). Based on the chronoamperometry curve, the catalytic active surface area was calculated to be 0.70 cm^2. Compared with the geometric area of 0.20 cm^2, the much higher catalytic active surface area indicated that the electrode effective surface area was increased obviously after the SN-AW modification, which would increase the electrochemical active site and enhance the electrochemical response.

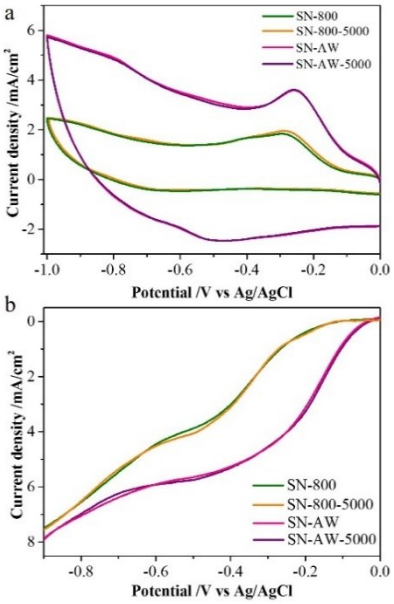

Fig. S6 CV (a) and LSV (b) curves of the as-synthesized SN-800 and SN-AW in O_2 saturated 0.1 M KOH solutions. The SN-800-5000 and SN-AW-5000 represents the curves after continuous cycling of 5000 cycles.

Similar to the superior stability of the SN-AW indicated by the chronoamperometric measurements (Figures 5a and 7a), the almost identical CV and LSV curves of SN-AW electrode before and after the continuous potential further confirmed it long-term operation stability and reusable (Figure S6). This higher stability is attributable to the improved chemical stability achieved by the acid washing process, which can effectively prevent the loss of active sites. Compared with the CV and LSV curves of SN-800 before the continuous potential, a small positive shift of the ORR peak, onset potential, and current density was obtained after the 5000 cycles (Figure S6), indicated the slightly improvement of it electrocatalytic activity. This improvement might own to the partly leaching out of the ash content from SN-800 during the 5000 cycles, which would increase the electrocatalytic active contents of C, N, Fe and S.

Table S1. Properties of the as-synthesized sewage sludge-derived catalysts

	SN-800	SN-AW
S_{BET} (m^2/g)	111.12	265.05
total pore volume ($cm^3\ g^{-1}$)	0.14	0.34
average pore size (nm)[a]	4.91	5.11
conc. (wt %)		
C[b]	35.01	56.73
N[b]	1.40	1.84
S[c]	0.64	0.45
Fe[d]	15.16	9.94
Si[c]	2.13	7.06
Al[d]	3.57	1.42
Mg[d]	0.93	0.24
Ca[d]	3.80	0.36
Cr[d]	0.05	0.03
Mn[d]	0.18	0.06
Ni[d]	0.64	0.49
Cu[d]	0.11	0.16

[a]: Calculated from the Barrett-Joyner-Halenda equation using the desorption isotherm.

[b]: The contents of C, N, and S were obtained by Elemental Analyze.

[c]: The content of Si was obtained by EDX.

[d]: The content of metals was obtained by ICP.

Table S2. Comparison of the synthesis catalytic activity of different catalysts

Starting materials	Synthesis process	Catalyst	Surface area	Electrolyte		OER	Reference
				0.1M KOH	Acidic media		
Sewage sludge	800 °C for 2 h in NH_3, HCl washed	N, Fe, and S multi-doped carbon	265.1	comparable with Pt/C	comparable with Pt/C	Yes	**This work**
Sewage sludge	500-900 °C for 2 h in N_2	N, Fe-doped carbon	44	unknown	unknown	unknown	*Bioresource Technol.* 2013, 144, 115
Surplus sludge	400-900 °C for 2 h in N_2, 40% HF washed	N-doped carbon	310.8	lower than Pt/C	unknown	unknown	*ACS Appl. Mater. Interf.* 2014, 6, 14911
Sewage sludge coconut shell	900 °C for 2 h in N_2	N, Fe and P and contents	92	comparable with Pt/C	unknown	unknown	*J. Mater. Chem. A* 2015, 3, 8475
Municipal sludge	900 °C for 2 h in N_2, 40% HF washed	Anode	unknown	unknown	unknown	unknown	*J. Power Sources* 2016, 307, 105

Ginkgo leaves	1000 °C for 1 h in NH_3	N-doped carbon nanosheets	1436.0	comparable with Pt/C	unknown	unknown	*J. Power Sources* 2014, 272, 8
Typha orientalis	Hydrothermal 180 °C for 12 h, 800 °C for 2 h in NH_3	N-doped carbon nanosheets	898	comparable with Pt/C	lower than Pt/C	unknown	*Energy Environ. Sci*. 2014,7, 4095
Bacterial cellulose	700-900 °C for 1 h in NH_3	N-doped carbon nanofiber	916	comparable with Pt/C	unknown	unknown	*Nano Energy* 2015, 11, 366
Ginkgo leaves	800 °C for 2 h in N_2, HCl washeds	N-doped carbon shell	583.1	comparable with Pt/C	unknown	unknown	*Nano Energy* 2015, 13, 518
Honeysuckles	800 °C for 2 h in N_2, HCl washed	S, N co-doped carbon	802.8	comparable with Pt/C	unknown	unknown	*Nano Energy* 2015, 12, 785
Enoki mushroom	ball-milling with carbon nanotubes for 5 h, 900 °C for 2 h	N-doped carbon	305.3	comparable with Pt/C	lower than Pt/C	unknown	*Nanoscale* 2015, 7, 15990

Dopaminehy drochloride ammonia iron acetate	Dopaminehy drochloride mixed with ethanol and ammonia, proceed for 30 h, stirring iron acetate overnight, 800 ^{o}C for 1 h in Ar, H_2SO_4 washed	Fe@Fe_3C/C-N-doped carbon spheres	2006	comparable with Pt/C	comparable with Pt/C	unknown	*Adv. Mater*. 2013, 25, 998
$La(NO_3)_3 \cdot 6H_2O$, $Sr(NO_3)_2$, $Co(NO_3)_2 \cdot 6H_2O$ and $Fe(NO_3)_3 \cdot 9H_2O$ in H_2O, C_2H_5OH	Synthesis of $La_{0.5}Sr_{0.5}Co_{0.8}Fe_{0.2}O_3$ catalyst, Synthesis of N-doped reduced graphene oxide	$La_{0.5}Sr_{0.5}Co_{0.8}Fe_{0.2}O_3$ combined with N-doped reduced graphene oxide	unknown	comparable with Pt/C	unknown	Yes	*Nano Energy* 2014, 10, 192–200

and DMF, PVP, graphene oxide							
Prussian blue	750-1050 ^{o}C for 2 h, HCl washed	Fe/Fe_3C nanoparticle encapsulated N-doped graphitic	unknown	comparable with Pt/C	unknown	Yes	*Green Chem*. 2016, 18, 427
carbon nanotube, graphene	modified Hummers' method, 900 °C annealed in 2 torr of 10% NH_3/argon at for 30 min…	carbon nanotube–graphene complexes	unknown	comparable with Pt/C	comparable with Pt/C	unknown	*Nature Nanotech*. 2012, 7, 394